Seedling Project Report:
A Novel Heat Pump Integrated Underground Thermal Energy Storage for Shaping Electric Demand of Buildings

Xiaobing Liu
Ming Qu
Liang Shi
Joseph Warner

May 2019

OAK RIDGE NATIONAL LABORATORY
MANAGED BY UT-BATTELLE FOR THE US DEPARTMENT OF ENERGY

Building Equipment Research Group

SEEDLING PROJECT REPORT:
A NOVEL HEAT PUMP INTEGRATED UNDERGROUND THERMAL ENERGY
STORAGE FOR SHAPING ELECTRIC DEMAND OF BUILDINGS

Xiaobing Liu (Oak Ridge National Laboratory)
Ming Qu (Purdue University)
Liang Shi (Purdue University)
Joseph Warner (University of Tennessee)

May 2019

CONTENTS

LIST OF FIGURES

LIST OF TABLES

ACKNOWLEDGMENTS

EXECUTIVE SUMMARY

The beneficial electrification ongoing in many aspects of our society results in a continuous increase in the demand for electricity. However, the capacity of existing electric grids is limited, and intermittent outputs from rapidly growing renewable power generation capabilities (e.g., solar, wind) pose unique challenges to balancing supply and demand on the national grid. When renewable power produces more energy than that can be used at one time, grid operators curtail renewable power, reducing its economic and environmental benefits. On the other hand, electricity generators need to be able to quickly ramp up energy production when the contribution from renewable power falls (e.g., when sun sets or the wind stops). Buildings are the primary users of electricity: 75% of all US electricity is consumed within buildings, and building energy use drives 80% of peak electric demand (EIA 2018). 40–70% energy consumption in buildings is for thermal loads, including space heating, space cooling, and water heating. Integrating thermal energy storage with existing electric grids has the potential to address the challenges we face as a nation by providing the flexibility of shifting or leveling the demand for electricity at buildings, therefore improving the stability of the grid and deferring the need for increased power generation capacity.

The objective of this seedling project is to preliminarily assess the technical feasibility of utilizing underground thermal energy storage (UTES) and electric-driven heat pumps (EDHPs) to enable flexible behind-the-meter electric demand of buildings while meeting their thermal demands in an energy-efficient manner. With a combined EDHP+UTES system, overproduced renewable power or the electricity generated at off-peak hours can be used to produce useful thermal energy to be stored in the UTES. The stored thermal energy is later utilized directly or through an EDHP to meet buildings' thermal demands during peak hours. Because UTES is underground, it can utilize geothermal energy by enabling geothermal heat pumps, which can meet thermal demands with higher efficiency than conventional space heating and cooling technologies. The EDHP+UTES system, therefore, not only shapes electric demand but also saves energy due to its higher efficiency.

A novel UTES technology, the dual-purpose underground thermal battery (DPUTB), was invented at Oak Ridge National Laboratory (ORNL) in collaboration with Purdue University under this seedling project. It is the key component of the proposed EDHP+UTES system. The DPUTB innovatively integrates a ground heat exchanger and underground thermal energy storage. It is designed to incorporate phase change materials, a dual-source heat pump system and a model-based predictive smart control to enable flexible behind-the-meter electric load and to bridge the intermittent renewable power supply and the fluctuating thermal loads of a building without increasing energy consumption.

A small-scale prototype of the DPUTB has been built and tested at ORNL. A 1D model of the DPUTB has been developed to simulate its performance under various operating conditions. The model was validated against the measured performance data of the small-scale prototype. The experimentally validated DPUTB model was then coupled with a building energy supply system, which included a dual-source heat pump (DSHP) and a building, to study the load shifting performance and energy consumption of the proposed system.

Simulation results indicate that an integrated system using the DPUTB with a DSHP can shift or level the electric load of a typical residential building in summer and reduce the electric demand during peak hours by 37% on a typical summer day. The DPUTB also works as a low-cost ground heat exchanger to provide a favorable entering water temperature for the more efficient operation of the heat pump. As a result, the integrated system also reduces the daily power consumption of the building by 11% compared with conventional heating, ventilation, and air conditioning systems. When deployed at large scale, the integrated DPUTB and DSHP system can help mitigate the growing burden on the existing electric grids,

especially the duck-curve effect resulting from increasing penetration of the intermittent renewable power generation.

The following supporting data have been submitted to the US Department of Energy Geothermal Data Repository:

1. Lab test results of a small-scale prototype DPUTB
2. A numerical model of DPUTB
3. Mid-term review presentation
4. Technical report and associated technical papers

1. INTRODUCTION

The increasing electricity generation from renewable energy (e.g., solar, wind) in recent years raises a challenge to the existing electric grid due to its intermittent outputs. The duck-curve phenomenon shown in Figure 1 reflects this mismatch between the renewable power supply and the demand from the grid. It will cause the electric generator to work in an unstable condition, resulting in lower efficiency and a shorter lifespan for the power plant. On the other hand, the increasing penetration of renewable power generation would lead to excess power production during its peak generation period and thus needs to be curtailed. However, this limits the use of renewable power.
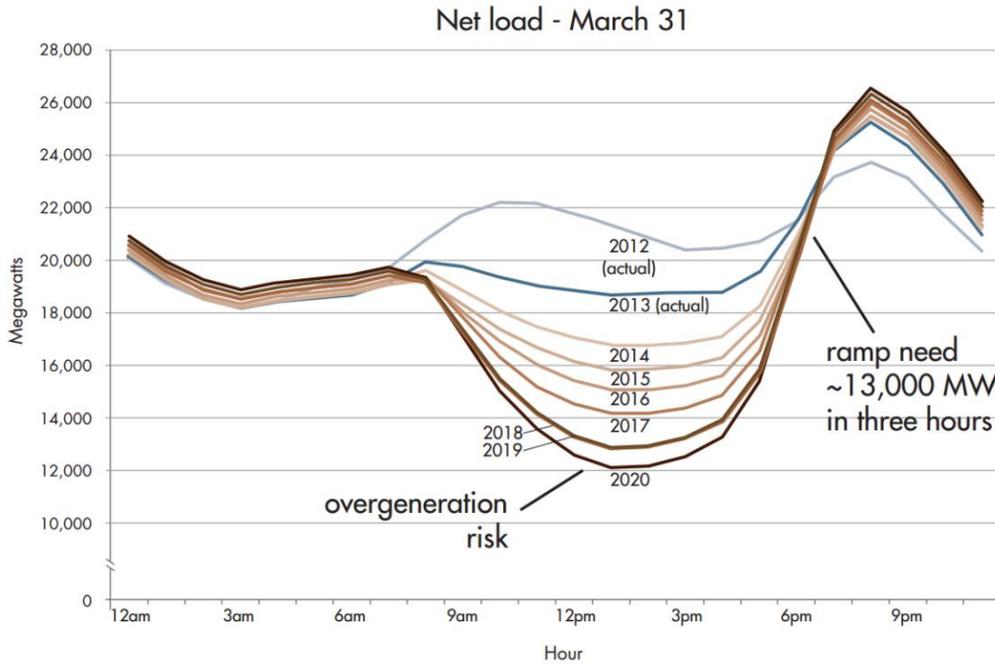
Figure 1. Duck curve of electricity demand due to intermittent renewable power (CAISO 2013).

Meeting the increasing demand for electricity with the existing grid assets and the growing intermittent renewable energy supply poses a big challenge to US energy systems. Buildings are the primary users of electricity: 75% of all US electricity is consumed within buildings, and building energy use drives 80% of peak electric demand (EIA 2018). 40–70% energy consumption in buildings is for thermal loads, including space heating, space cooling, and water heating. Integrating thermal energy storage with the electric grids has the potential to address the challenge by providing flexibility to shift or level the demand for electricity at buildings, therefore improving the stability of the grid and deferring the need to increase power generation capacity.

One possible method to shift peak power consumption is to pre-cool or pre-heat the building thermal mass. The advantage of this technique is that it requires no additional mechanical equipment (Turner et al. 2015). Pre-cooling and pre-heating strategies are usually applied in office buildings due to their high thermal mass. However, systems or materials can also be added to thermally light buildings (Olsthoorn et al. 2017). Several residential applications also exist for peak shaving and shifting. Turner et al. investigated a prototype residential building in 12 different climate zones and indicated a potential of up to 50% peak shaving by varying the heating, ventilation, and air conditioning (HVAC) system set point for the pre-cooling approach. In some cases, the pre-cooling strategy led to a high shaving effect up to 99% of the load during on-peak periods. However, the researchers also questioned if this is reasonable if

pre-cooling would significantly increase the total cooling load, sometimes by as high as a 67% increase (Turner et al. 2015). Cetin et al. focused their study on residential buildings with smart thermostats that can automatically set back the thermostat of the HVAC during on-peak periods and found that doing so would reduce electric grid demand as well as thermal energy consumption. Their results showed that the set point temperature was an important influencing factor in all climate zones. A 1° increase in set point temperature decreased the HVAC energy use by 24%, 17%, and 9% in climate zones 4a, 3a, and 2b (Cetin et al. 2016). Bojić and Yik studied how changes in the fabric constructions would affect the yearly and peak cooling demand of the building under Hong Kong's climatic conditions. The results showed that adding insulation to the envelope and partitions would reduce the yearly space cooling load by up to 38% but could either increase or reduce the peak cooling demand depending on the number and position of the insulation layer in the walls. Their results also indicated that reducing the thermal capacity of the envelope and partitions would lead to significant increases in the peak cooling demand, by more than 60% in the extreme case (Bojić and Yik 2005). Dominković et al. investigated the potential of thermal building mass for storage in district heating systems in Sønderborg, Denmark. The study showed that longer pre-heating time increased the possible duration of cut-off events. The result indicated that flexible load accounts for 5.5% to 7.7% of the total district heating demand (Dominković et al. 2018).

Another approach to storing thermal energy for demand-side flexibility is to incorporate storage tanks into building energy supply systems. Hirmiz et al. used a numerical model to investigate the feasibility of integrating phase change material (PCM) thermal storage into heat pump systems to assist demand-side management. The results showed that thermal energy storage could completely offset peak demand periods with sufficient storage volumes. However, water-only storage volumes can be huge. A hybrid PCM water tank with 75% PCM could reduce storage volume by up to threefold compared to water-only storage. The researchers concluded that thermal storage was not an energy-efficient solution and would generally lead to an increase in the overall electric consumption over a day (Hirmiz et al. 2019). Martin et al. studied direct-contact PCM–water cold storage for peak shaving. Experimental and simulation results showed that the storage capacity for cold is said to be 12 kWh/m^3 for water, 25–60 kWh/m^3 for PCM, and over 73 kWh/m^3 for ice. According to the authors, the low cooling power and insufficient heat transfer in PCM are considered the most significant barriers to applying PCM for TES (Martin et al. 2010).

Romanchenko et al. compared the two possible methods for building load shifting by using a hot water tank and the thermal inertia of buildings. They investigated the benefits of applying thermal energy storage in district heating systems in Sweden to decrease heating load variations. Their results showed that both the hot water tank and the thermal inertia of buildings benefited the operation of the district heating system. However, the hot water tank stored more than twice as much heat over the modeled year compared to the thermal inertia of buildings, and it could be used to store heat for a period longer than a few days. Moreover, the hot water tank had its full capacity available for charging and discharging at all times, while the capacity of the thermal inertia of buildings depended on the heat transfer between the building core and its indoor conditions (Romanchenko et al. 2018).

The objective of this seedling project is to preliminarily assess the technical feasibility of utilizing underground thermal energy storage (UTES) and electric-driven heat pumps (EDHPs) to enable flexible behind-the-meter electric demand of buildings while meeting their thermal demands in an energy-efficient manner. With a combined EDHP+UTES system, the overproduced renewable power or the electricity generated at off-peak hours can be used to produce useful thermal energy to be stored in the UTES as shown in Figure 2a. The stored thermal energy is later directly utilized as shown in Figure 2b or through an EDHP to meet buildings' thermal demands during the grid's peak hours. Because UTES is underground, it can utilize geothermal energy through geothermal heat pumps (GHPs), which can meet the thermal demands with higher efficiency than conventional space heating and cooling technologies. The EDHP+UTES system, therefore, not only shapes the behind-the-meter electric load profile of the building but also saves energy due to its higher efficiency.
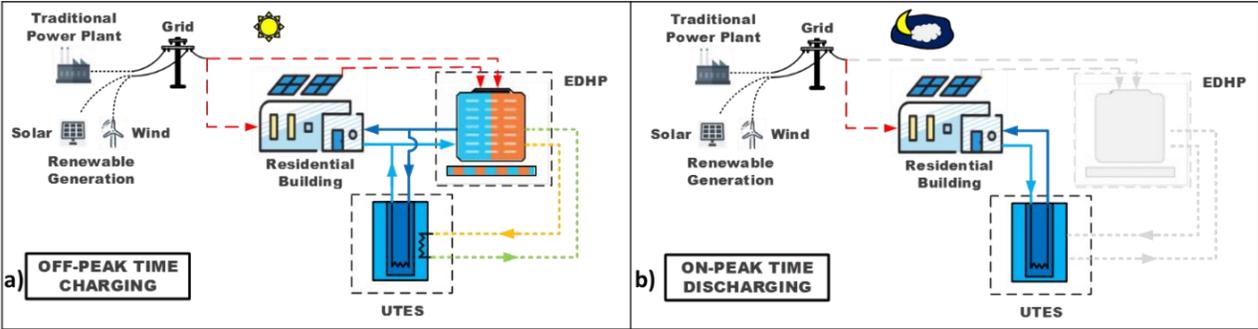
Figure 2. Schematic of the EDHP+UTES system: (a) EDHP operates to cool a building and also to store cooling energy in a UTES during off-peak hours; (b) stored cooling energy in the UTES is discharged to cool the building with little electricity consumption during peak hours.

2. DUAL-PURPOSE UNDERGROUND THERMAL BATTERY

A novel UTES technology, the dual-purpose underground thermal battery (DPUTB), was invented by Oak Ridge National Laboratory (ORNL) in collaboration with Purdue University under this seedling project. It is the key component of the proposed EDHP+UTES system. The DPUTB innovatively integrates a ground heat exchanger and underground storage for the dual purposes of heat exchange and energy storage (Patent pending DOE S# S-138,992). It is designed to incorporate PCMs, heat pump systems, and model-based predictive smart control for enabling behind-the-meter energy storage and electric load shifting, as well as bridging between the intermittent renewable power supply and buildings' fluctuating thermal demand without increasing energy consumption.

The EDHP+UTES system uses a dual-source heat pump (DSHP) that utilizes either the ambient air or the ground source as its heat sink and heat source. The DSHP uses ambient air as its heat sink when the ambient air temperature is low. On the other hand, it uses the ground as the heat sink and heat source to efficiently provide cooling or heating either directly to the building or be stored in UTES, as shown in Figure 2b.

A small-scale prototype of the DPUTB has been built and tested at ORNL. As depicted in Figure 3, the DPUTB consists of an enclosed inner tank within a larger water tank. A customized PCM is wrapped on the outer surface of the inner tank. Because of the PCM's low thermal conductivity, especially during the phase change process, it serves as insulation to block the heat transfer between the inner and outer tanks. Another type of PCM, having a different melting temperature from the PCM used in the wall of the inner tank, is applied in the inner tank for storing the cooling or heating energy released from the inner tank. Two heat exchangers are installed in the inner and outer tanks, respectively, to exchange heat with an HVAC system. This design allows for storing chilled water or ice in the inner tank and later for providing direct cooling to eliminate or reduce the electricity required by the heat pump during the electric grid's peak hours. The annulus of the DPUTB (i.e., space below the inner and outer tanks) is designed as a ground heat exchanger, not only to exchange heat with the surrounding ground formation but also to recover energy losses from the inner tank for the more efficient operation of the heat pump system.
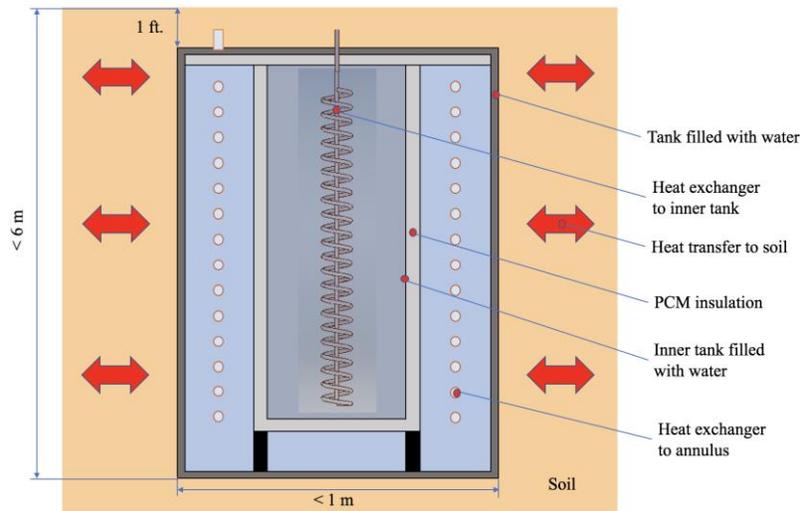
(a)
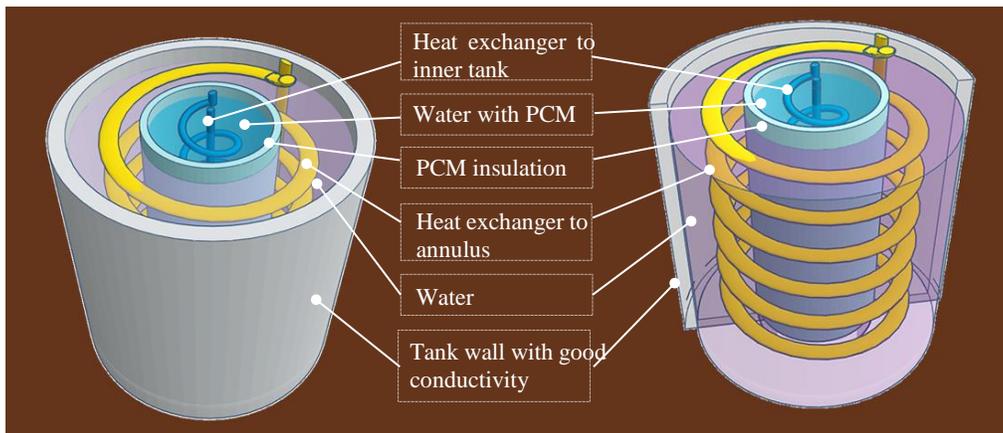
(b)

Figure 3. Schematic of the dual-purpose underground thermal battery: (a) a sectional view; (b) a 3D rendering. (Patent pending DOE S# S-138,992)

The DPUTB incorporated with the DSHP can operate in multiple modes, as shown in Figure 4. During the off-peak period and when no renewable power is available (e.g., at night), the heat pump runs on air source at full capacity (Figure 4a). During the off-peak period and when there is an overproduction of renewable power, the heat pump runs at its full capacity. During this period, if the heat pump capacity is higher than the building's thermal demand (Figure 4b), thermal energy will be stored in the inner tank of the DPUTB. If the heat pump capacity is lower than the building's thermal demand (Figure 4c), the stored thermal energy in the DPUTB will be discharged to meet the thermal demand. During peak hours, the heat pump is turned off, and the stored thermal energy in the DPUTB is used to provide direct cooling and heating to the building (Figure 4d). Once the stored thermal energy is insufficient to meet thermal demand, the DSHP is switched to the ground source (i.e., the annulus of the DPUTB) to meet the building's thermal demand at high efficiency (Figures 4b and 4d).
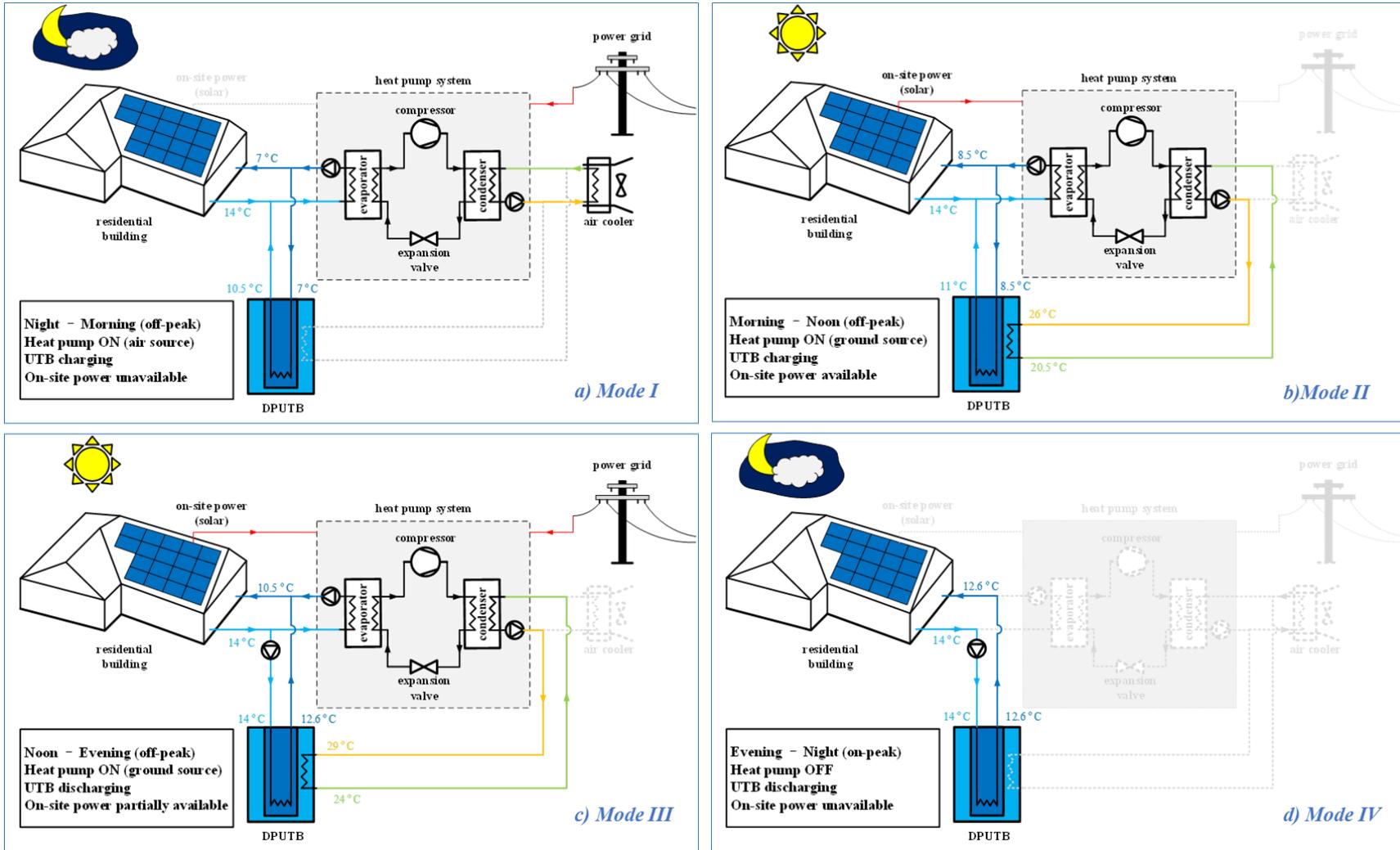
Figure 4. Multiple operating modes of the DPUTB incorporated with the DSHP.

3.   DEVELOPMENT AND LAB TEST OF A SMALL-SCALE PROTOTYPE DPUTB

A small-scale prototype of the DPUTB was built at ORNL (Figure 5). The diameter and depth are scaled down with a 1:5 ratio from that of a full-scale DPUTB. The dimensions of the small-scale DPUTB prototype are listed in Table 1, along with the thermal properties of the PCM used in the prototype. The water tank of the small-scale prototype is made with PVC, and the thickness of the tank wall is 8.2 mm. A helical heat exchanger made with a 6.4 mm diameter copper tube is placed at the center of the tank and enclosed with a 10.7 cm diameter plastic tube. The plastic tube is sealed at the bottom to form an inner tank. The inner tank is filled with water. Three PCM panels curved into a hollow-cylinder shape are wrapped around the entire length of the inner tank (including top and bottom). The thickness of each PCM panel is 3.81 mm. The PCM is made with a mixture of salt hydrates and has a melting point of 23°C.
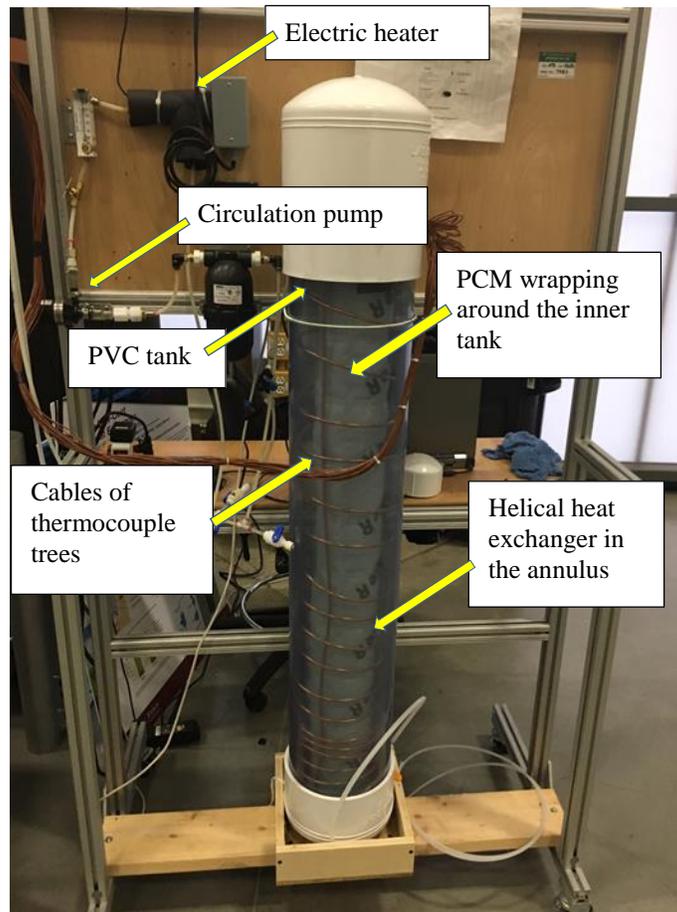
Figure 5. A small-scale prototype of the dual-purpose underground thermal battery.

Table 1. Dimensions and thermal properties of the small-scale DPUTB prototype.

Dimension	Value	Unit	PCM properties	Value	Unit
Inner tank diameter	7.79	cm	Melting point	23	°C
Inner PVC shell thickness	0.55	cm	Heat of fusion	160	kJ/kg
PCM blanket thickness	2.54	cm	Thermal conductivity (solid)	0.1489	W/m K
Outer tank diameter	20.27	cm	Thermal conductivity (liquid)	0.1596	W/m K
Outer PVC shell thickness	0.82	cm	Specific heat (solid)	3000	J/kg K
Height of the inner tank	121.92	cm	Specific heat (liquid)	2740	J/kg K
Height of the outer tank	121.92	cm			

The small-scale DPUTB prototype was tested in a chamber with controlled climate using an existing test facility at ORNL. Figure 6 shows the schematic of the test facility, which includes a circulating pump, an electric heater, a refrigerated circulating water bath, and a data acquisition system.
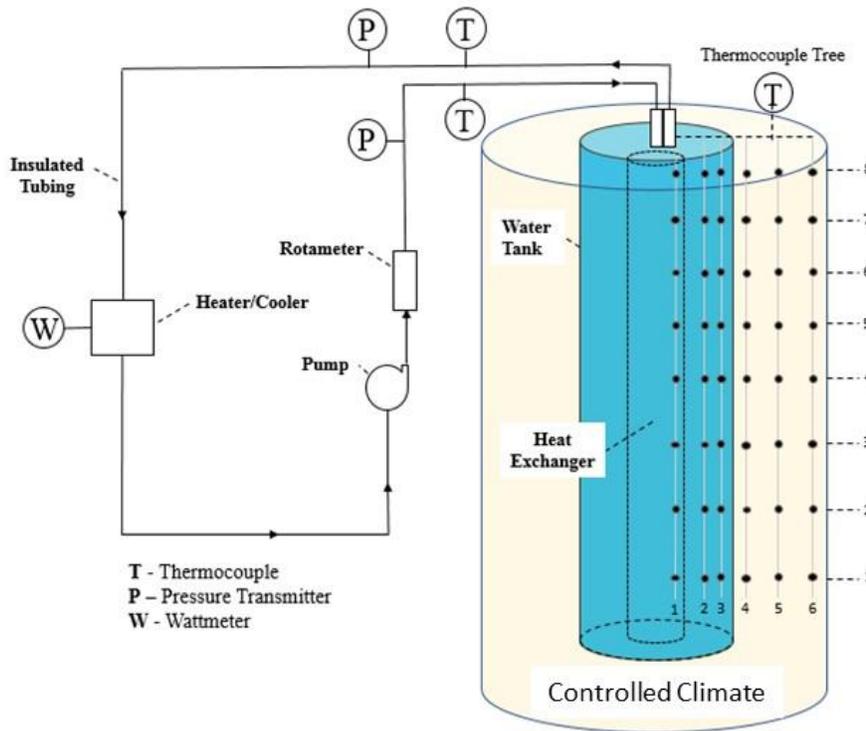
Figure 6. Schematic of the experimental apparatus for testing a small-scale DPUTB.

The pump circulates water in the helical heat exchanger at a constant flow rate. The heater provides constant heat input to either the inner tank or the annulus of the DPUTB at a predefined schedule to emulate heat rejection load. The water bath provides chilled water at a constant temperature to either the inner tank or the annulus of the DPUTB at a predefined schedule to emulate cooling inputs. The data acquisition system records the following measurements at 1 min intervals.

- Flow rate, inlet, and outlet temperature, and differential pressure of the helical heat exchanger in the inner tank.

- Flow rate, inlet, and outlet temperature, and differential pressure of the helical heat exchanger in the annulus.

- Temperatures at various locations inside the DPUTB. The temperature sensors are suspended vertically in six groups. The first group is inside the inner tank; the second is in the middle of the annulus; the third is on the inside wall of the DPUTB. The other three groups of temperature sensors are not used in the lab test.

Lab test results for the prototype DPUTB are shown in Figure 7. During the test the inner tank water was charged for 6 h with the water bath circulating a mixture of water and glycol at around 0 °C with a 26.5 kg/h flow rate through the heat exchanger in the inner tank (HX 1), which was intended to store cooling energy (mode 1). In the following 2 h, the water bath was turned off, and the inner tank was heated up by the electric heater with a constant 70 W heat input, which was intended to emulate the discharging operation for directly cooling the building without running the heat pump (mode 2). In the last 6 h of the test, HX 1 was turned off, and 70 W heat was rejected to the annulus intermittently (switching on and off at 15 min intervals) through the second heat exchanger in the annulus (HX 2) to emulate the heat rejection from a GHP (mode 3). The lab test results indicate that the inner tank temperature can be cooled down to around 2–3°C in less than 2 h, and the low temperature was maintained for the rest 4 h while the water temperature in the annulus dropped only slightly from its initial temperature (16.5°C) during the 6 h charging operation. The water temperature in the inner tank increased to about 16.5°C after the 2 h discharging period, and the outlet fluid temperature from HX1 (T_out_HX1) was less than 1°C higher than the inner tank water temperature. In the mode 3 operation, the inner tank water temperature rose slowly and eventually merged with the annulus water temperature. The outlet fluid temperature of HX2 (T_out_HX2) was nearly identical to the annulus water temperature. T_out_HX2 was less than 20°C during the 6 h heat rejection operation, which would have led to high operational efficiency of a GHP system.
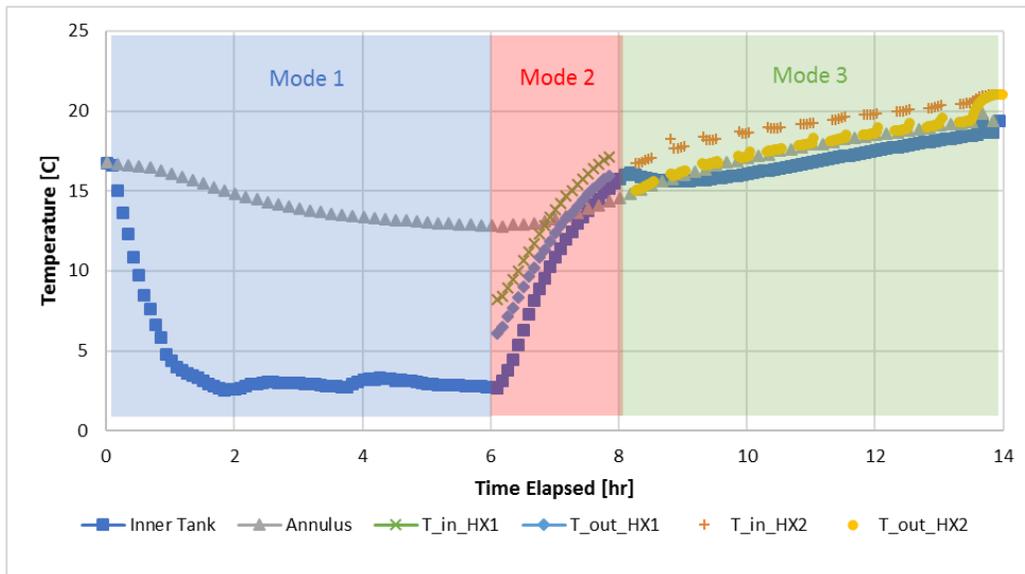
Figure 7. Lab test results for the small-scale prototype DPUTB operated in three modes: (1) charging with cold water; (2) discharging with direct cooling; (3) discharging through a ground source heat pump.

The lab test results indicate that the current design allows for storing cooling energy in the DPUTB's inner tank without significant heat loss to the annulus. The low heat loss is due to the low thermal conductivity of the PCM wrapping around the inner tank, which served as insulation to reduce heat

transfer between the inner tank and annulus, in addition to an energy storage medium for tempering the water temperature rise in the annulus when it was heated up beyond the PCM's melting point. The discharging performance in mode 2 (for direct cooling) needs to be improved to slow down the temperature rise of the inner tank. In the lab test, only water was filled in the inner tank, and the cooling water temperature was not below the freezing point; as a result, the water was not frozen during the charging process, and only the sensible heat of the water was used for providing direct cooling. If the inner tank were cooled down below the freezing point, or a PCM with a higher melting point than the freezing point of water were used, more cooling energy would have been stored in the inner tank and the temperature rise of the inner tank would have been slower. Figure 8 shows that ice was made on the heat exchanger in the inner tank when a coolant having a temperature of −2 °C was used to charge the inner tank.

Figure 8. Image of the inside of the small-scale prototype DPUTB showing ice formed on the heat exchanger in the inner tank when the coolant at −2 °C was used to charge the DPUTB.

4. NUMERICAL MODEL OF DPUTB

A 1D transient model has been developed in MATLAB to simulate the DPUTB's thermal response. The model is based on the following assumptions and simplifications:

- Only the heat transfer along the radial direction is accounted for.

- Tank water is well mixed due to natural convection (i.e., tank water is isothermal).

- Thermo-physical properties of the soil are homogeneous, and the heat transfer in the simulation domain is symmetric.

- Convection heat transfer in the liquid PCM is neglected, and only the conduction heat transfer is modeled.

- The PCM's freezing point is identical to its melting point.

- Heat exchange through the top and bottom surfaces of the DPUTB is neglected.

4.1 SIMULATION DOMAIN

The simulation domain of the 1D DPUTB model is shown in Figure 9. The diameter of the simulation domain is 10 times that of the simulated DPUTB. Because the heat transfer within the soil will not go

beyond the boundary for short periods (e.g., a few months), an adiabatic boundary condition is applied to the perimeter of the simulation domain. The model accounts for the following heat transfer processes:

- Heat transfer between the heat exchanger in the inner tank (HX1) and the inner tank water,

- Heat transfer between the heat exchanger in the outer tank (HX2) and the outer tank water,

- Heat transfer between the inner and outer tank water through the inner tank wall (made with PVC) and the PCM wrapped around the inner tank,

- Heat transfer between the DPUTB shell and the surrounding soil,

- Phase change process within the PCM, and

- Phase change process within the inner tank.
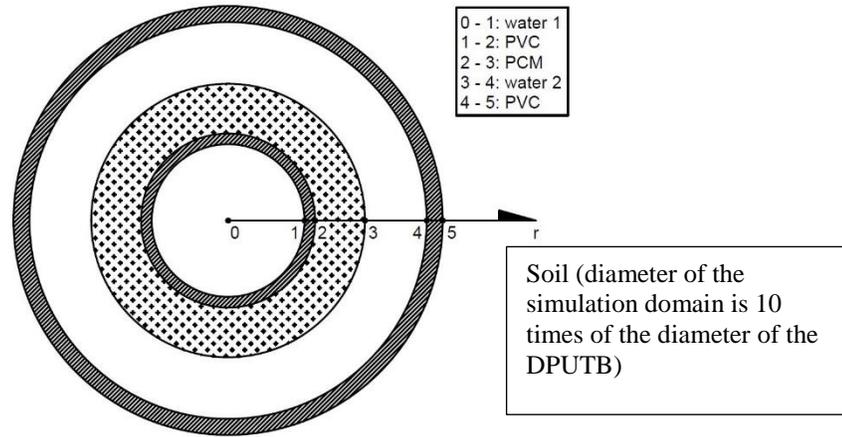
Figure 9. Simulation domain of the 1D model of DPUTB.

4.2 GOVERNING EQUATIONS

4.2.1 Heat Exchanger Modeling

HX1 and HX2 are heat exchangers that directly interact with the inner and outer tank water. The input thermal energy to the tank water can be determined by the heat transfer coefficient and the surface area of the heat exchanger, inlet fluid temperature of the heat exchanger, the tank water temperature, and the mass flow of the fluid in the heat exchanger, as expressed in Eq. 1:

$$q = UA \cdot \Delta T_{lm}, \tag{1}$$

where q is the heat exchange rate, U is the heat transfer coefficient of the heat exchanger, A is the surface area of the heat exchanger, and ΔT_{lm} is the logarithm mean temperature difference between the fluid in the heat exchanger and the tank water at a given time step, which is expressed as Eq. 2.

$$\Delta T_{lm} = \frac{(T_{HEX,in}-T_{tank})-(T_{HEX,out}-T_{tank})}{\ln\frac{T_{HEX,in}-T_{tank}}{T_{HEX,out}-T_{tank}}}, \tag{2}$$

where $T_{HEX,in}$ is the inlet temperature of the heat exchanger, $T_{HEX,out}$ is the outlet temperature of the heat exchanger, and T_{tank} is the tank water temperature.

At steady state, the heat exchange rate is also equal to the enthalpy change of the fluid in the heat exchanger, which can be calculated with Eq. 3:

$$q = \dot{m}_{HEX} \cdot c_p \cdot (T_{HEX,in} - T_{HEX,out}), \tag{3}$$

where $\dot{m}_{HEX}$ is the mass flow of the heat carrier fluid in the heat exchanger and c_p is the specific heat of the heat carrier fluid.

The above equations are solved iteratively to determine the heat exchanger outlet temperature and the heat transfer rate at a given time step. The calculated heat transfer rate is used as a boundary condition of the DPUTB model.

4.2.2 Natural Convection Modeling

To determine the convection heat transfer coefficient between the tank water and its surrounding solid surfaces, the Rayleigh number and the Nusselt number are calculated with Eq. 4 and Eq. 5, respectively:

$$\text{Ra} = \frac{g \cdot \beta \cdot |T_s - T_\infty| \cdot L^3}{v \cdot \alpha}, \tag{4}$$

where g is the gravity, β is the coefficient of thermal expansion of the fluid, T_s is the surface temperature, T_∞ is the fluid bulk temperature, L is the characteristic length, v is the kinematic viscosity, and α is the thermal diffusivity of the fluid.

$$\text{Nu} = \left\{ 0.825 + \frac{0.387 \cdot \text{Ra}^{\frac{1}{6}}}{\left[1 + (0.492/Pr)^{\frac{9}{16}} \right]^{\frac{8}{27}}} \right\}^2, \tag{5}$$

where Pr is the Prandtl number of the fluid.

The convective heat transfer coefficient can be determined with Eq. (6):

$$h_{conv} = \text{Nu} \cdot \frac{k}{L}, \tag{6}$$

where k is the thermal conductivity of the fluid.

The surface temperature can be calculated based on the energy balance at the surface:

$$h_{conv} \cdot (T_\infty - T_s) = \frac{k_{other}}{\Delta x} \cdot (T_s - T_{other}), \tag{7}$$

where k_{other} is the thermal conductivity of the material on the other side (either PCM or tank wall).

Equations (4)–(7) are solved iteratively to determine the surface temperature of the solid surface at a given time step.

4.2.3   Conduction Heat Transfer

The PCM and soil are discretized into a series of small cells along the radial direction, and the conduction heat transfer equation is applied to each cell to determine its average temperature. For 1D heat conduction in the cylindrical coordinates, the conduction heat transfer equation can be expressed as Eq. (8):

$$\frac{1}{r}\frac{\partial}{\partial r}\left(r \cdot k \frac{\partial T}{\partial r}\right) = \rho \cdot c_p \frac{\partial T}{\partial t},\tag{8}$$

where r is the radial position of the cell and ρ is the density of the material within the cell.

For explicit numerical calculations, the heat equation can be discretized into the following expression, as expressed in Eq. (9):

$$\rho \cdot c_p \frac{T_i^{new}-T_i}{\Delta t} = \frac{1}{r_i}\cdot\frac{r_{i+\frac{1}{2}}\cdot k_{i+\frac{1}{2}}\frac{T_{i+1}-T_i}{\Delta r}-r_{i-\frac{1}{2}}\cdot k_{i-\frac{1}{2}}\frac{T_i-T_{i-1}}{\Delta r}}{\Delta r},\tag{9}$$

Where the subscripts denote the position and the superscripts denote the time step. Applying this equation to each cell gives the temperature profile of the soil and PCM at a given time step.

4.2.4   Phase Change Modeling

The latent heat accumulation method (Muhieddine et al. 2009) is applied to simulate the phase change process within the PCM and the inner tank (filled with water or another PCM). During the phase changing period, the temperature of the PCM is fixed, but the latent heat within the PCM mass changes. For a certain amount of PCM, the maximum latent heat it can store can be calculated as:

$$Q_{latent,max} = m \cdot \Delta H,\tag{10}$$

where m is the mass of the PCM and ΔH is the heat of fusion.

If the PCM is in a solid or liquid phase, no latent heat is involved in the heat transfer process. When a PCM cell (finite control volume) is frozen (i.e., from liquid to solid), a "solid fraction" parameter is defined based on how much latent heat is accumulated, and it is expressed with Eq. 11:

$$\theta = 1 - \frac{Q_{latent,acc}}{Q_{latent,max}},\tag{11}$$

where θ is the solid fraction and $Q_{latent,acc}$ is the amount of latent heat accumulated in the finite control volume. According to this definition, if the cell is all in the solid phase , $\theta = 1$, and if the cell is all in the liquid phase, $\theta = 0$. When the cell is in two-phase, θ ranges between 0 and 1, and it reflects how much solid is in the cell.

Within each time step, after the heat transfer calculation, the phase status of each cell is checked. Four scenarios are possible: two-phase melting, two-phase freezing, single-phase solid and single-phase liquid. If the cell is in a two-phase state, the cell should be tagged for further calculation. Take the melting scenario as an example, if the cell is tagged in melting, the cell temperature is reassigned to the melting point, and the latent heat increment is calculated from the fictitious sensible heat. The fictitious sensible heat is added to the accumulated latent heat storage of the cell for subsequent time steps until the accumulated latent heat equals the maximum latent heat available in the control volume. At this time step, the control volume becomes all liquid, the tag on the cell is removed, and the latent heat increment is no

longer calculated. The freezing scenario is of the same principle, and only the latent heat is inverted from storing to releasing.

4.3   COMPUTATIONAL METHOD

The explicit method is applied to solve the discretized heat transfer equations at each time step based on the temperature profiles of the soil and the PCM domains in the last time step and the tank water temperatures at the current time step. The explicit method is easy to conduct but certain stability confinement expressed with Eq. (12) should be satisfied:

$$d = \frac{\alpha \cdot \delta t}{(\delta r)^2} \leq 0.5, \tag{12}$$

where d is the stability determinant, α is the thermal diffusivity of the material, δt is the time increment, and δr is the radius increment of the cell.

4.4   MODEL VALIDATION

The lab test results presented in section 2 were used to validate the numerical model. For the current validation, three parameters—the ambient temperature, inlet temperatures from HX1, and inlet temperatures from HX2—were applied as the boundary conditions. The mass flow rates of HX1 and HX2 were constant during the whole experiment period, and their values were 26.5 kg/h. The UA values (i.e., the product of the heat transfer coefficient and the surface area) of the two heat exchangers are difficult to quantify due to the complicated geometry of the helical coil heat exchangers used in the prototype; therefore, it was estimated based on the typical UA value (5,000 W/°C) for similar heat exchangers.

With the abovementioned data as inputs of the numerical model, the model predictions and the experimental data show similar trends. However, the model predicted a lower inner tank water temperature during the first and third periods. It indicates that the model overestimates the insulation effect between the inner and outer tanks. The most plausible reason for this overestimation is that the PCM applied in the experiment consisted of three layers of commercially available PCM panels instead of the ideal one layer of PCM defined in the model. It is likely that some water flowed between the PCM panels in the lab test, which enhanced heat transfer. The enhanced heat transfer is equivalent to a much higher thermal conductivity of the PCM. Figures 10 and 11 show the comparison results after increasing the thermal conductivity of the PCM in the model from 0.15 to 0.60 W/m K. The simulation results resulting from increased thermal conductivity value of the PCM match well with the experimental data. The root square means error for the inner tank water temperature is 0.4°C, and for the outer tank water temperature is 0.8°C. It indicates that the numerical model can predict the performance of a DPUTB with reasonable accuracy.
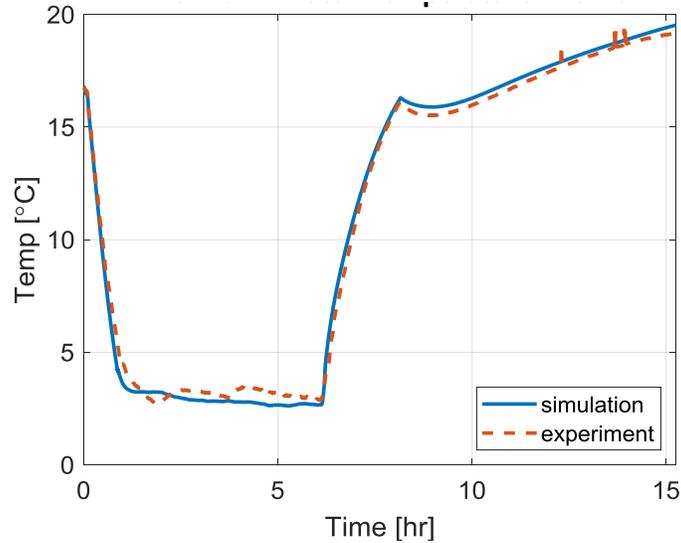
Figure 10. Comparison between measured and model-predicted inner tank water temperature of the small-scale prototype DPUTB (with increased thermal conductivity of PCM to account for possible water flow between the PCM sheets).
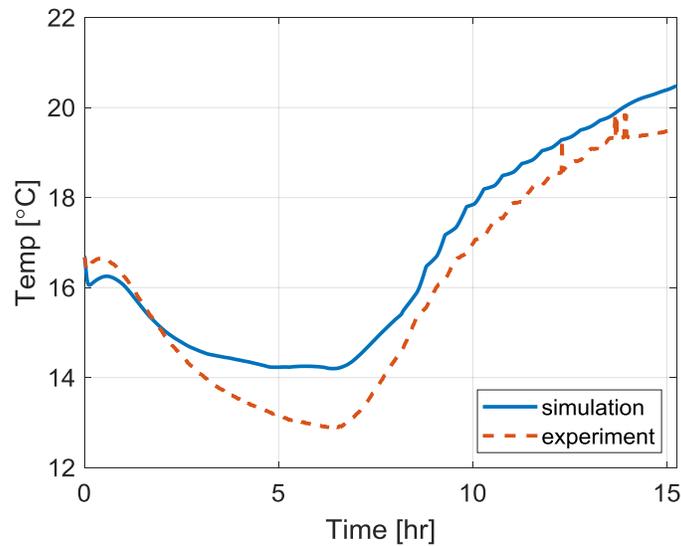
Figure 11. Comparison between measured and model-predicted water temperature in the annulus of the small-scale prototype DPUTB (with increased thermal conductivity of PCM to account for possible water flow between the PCM sheets).

5. PARAMETRIC STUDY FOR OPTIMAL CONFIGURATION OF DPUTB

The lab test and simulation results for the initial small-scale prototype DPUTB indicate that the discharging time is shorter than expected because of the inner tank's limited volume. The PCM inside the inner tank (water was used in the lab test) cannot wholly solidify after charging the DPUTB for a long period (e.g., 5 h) because the PCM wrapping around the inner tank is not a perfect insulation material, and therefore some of the cooling energy transfers to the annulus of the DPUTB during the charging process. This observation indicates the need for increasing the size of the inner tank and selecting a better PCM insulation.

14

On the other hand, the maximum diameter of the DPUTB is constrained by the capability of the inexpensive auger drill rig. Increasing the inner tank volume inevitably leads to a smaller annulus volume. The smaller annulus volume results in the less thermal capacity to temper the temperature change in response to heat rejection and heat extraction load of the GHP system, which leads to lower energy efficiency. Therefore, the design of the DPUTB must be optimized to achieving the desired discharging time, while retaining the GHP's high performance. The validated DPUTB model has been used for a parametric study to evaluate the impacts of various design parameters on the performance of the DPUTB, including thermal properties of PCMs, the thickness of the PCM panels, and the diameter of the inner tank.

5.1   INSULATION FOR THE WALL OF THE INNER TANK

The first simulation was performed to investigate the impact of increased thermal insulation between the inner tank and the annulus. In this simulation, a PCM with a very low thermal conductivity is applied to insulate the wall of the inner tank, and the thermal conductivity of the inner PVC wall is reduced to a minimal value. The simulation results show that increased thermal insulation leads to less heat transfer between the inner tank and the annulus, as shown in Figure 12a. Therefore, the inner tank water can even be cooled below the freezing point during a 5 h charging period. Figure 12b indicates that almost all the stored cooling energy is discharged during ~3 h later in the day.

(a) Water temperature   (b) Energy accumulation rate in the inner tank
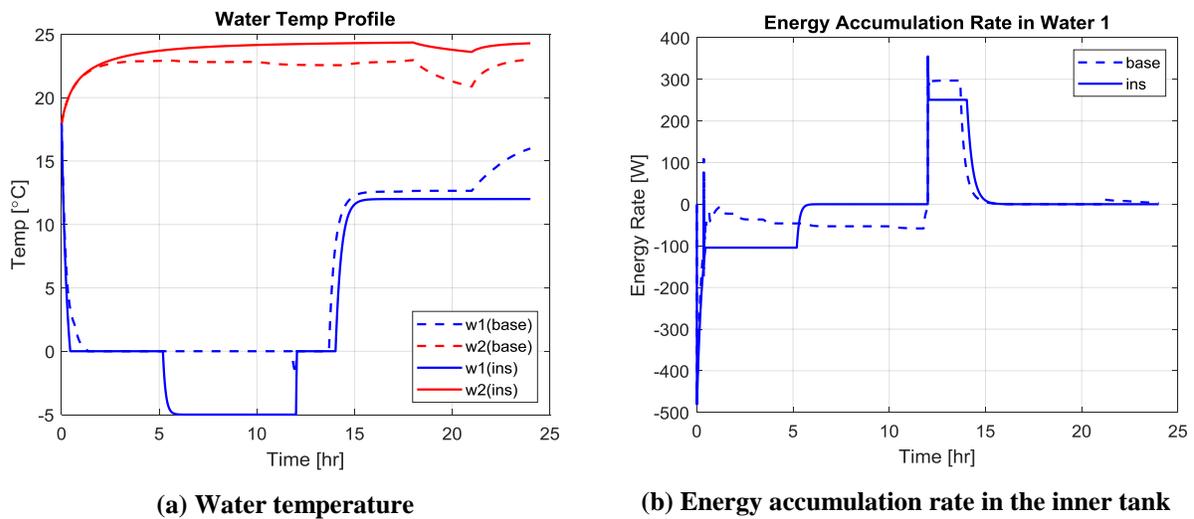
Figure 12. Temperature and energy comparison between the base case and the increased insulation case (W1: inner water; W2: annulus water; base: prototype; ins: increased insulation).

5.2   DIMENSION OF THE INNER TANK WITH INCREASED INSULATION

The second simulation was performed to investigate the impact of increased inner tank diameter on the overall performance of a DPUTB with increased insulation as discussed above. In this simulation, the diameter of the inner tank is twice its initial size. The simulation results show that by increasing inner tank volume, the thermal energy storage capacity of the DPUTB is increased approximately proportional to the square of the ratio of the diameter. The discharging period for providing direct cooling is increased as shown in Figure 13.

15
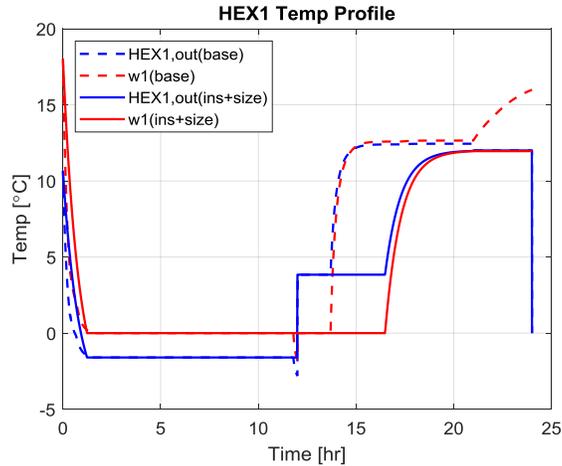
Figure 13. Comparison of the inner heat exchanger outlet fluid temperature: base case vs. insulation + large inner tank diameter (W1: inner water; HEX1: heat exchanger in the inner tank; base: prototype; ins+size: larger inner tank with increased insulation).

5.3 LARGE DIMENSION OF THE INNER TANK ONLY

The third simulation was performed to investigate the impact of increased inner tank diameter only on the overall performance of a DPUTB. In this simulation, the insulation of the inner tank is the same as that used in the prototype. The simulation results show that the inner tank with a doubled diameter can increase the discharging period by a factor of 3–4, although heat transfer still occurs from the inner tank to the annulus, as shown in Figures 14a and 14b, respectively.

(a) Temperature comparison of inner heat exchanger

(b) Energy accumulation rate in the inner tank
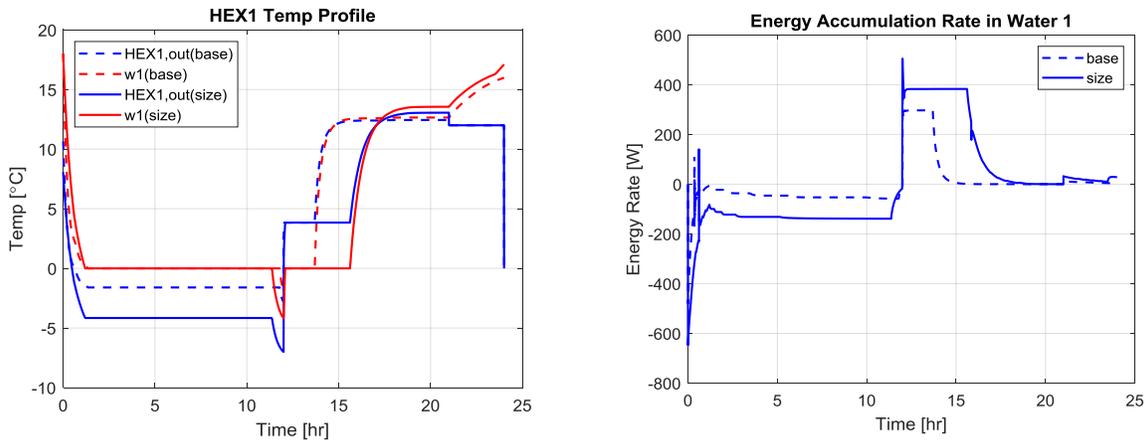
Figure 14. Comparison of temperature and energy between the base case and the case with larger inner tank diameter (W1: inner water; HX1: heat exchanger in the inner tank; base: prototype; size: larger inner tank).

This parameter study indicates that (1) the cooling energy storage capacity is proportional to the inner tank volume and (2) better insulation between the inner tank and the annulus would lead to more cooling energy stored and used late in the discharging period. It should be noted that the heat transferred from the inner tank to the annulus can still be useful since it can be recovered by the GHP, which uses the annulus of the DPUTB as its heat sink and heat source.

16

6. CASE STUDY OF SYSTEM PERFORMANCE OF THE DPUTB-DSHP SYSTEM

According to the US Information Administration (EIA 2018), buildings are the primary users of electricity: 75% of all US electricity is consumed within buildings, and building energy use drives 80% of peak electric demand. For residential buildings without onsite renewable power generation, the electric load profile on summer days typically has a peak in the late afternoon and a valley in the evening, as shown in Figure 15. This figure also shows that the peak electric demand is largely due to the operation of buildings' air conditioning systems in the late afternoon when the cooling load peaks. Buildings' high-peak electric demands stress the electric grid and may result in blackouts. It is thus highly desirable to level buildings' electric load profile so the electric grid's transmission and distribution capacity are fully utilized and the need for ramping up power generation during peak hours is avoided. A case study was performed through computer simulations to demonstrate the flexibility of shifting or leveling the electric load profile of a residential building by using a DPUTB integrated with a DSHP (i.e., a DPUTB-DSHP system).
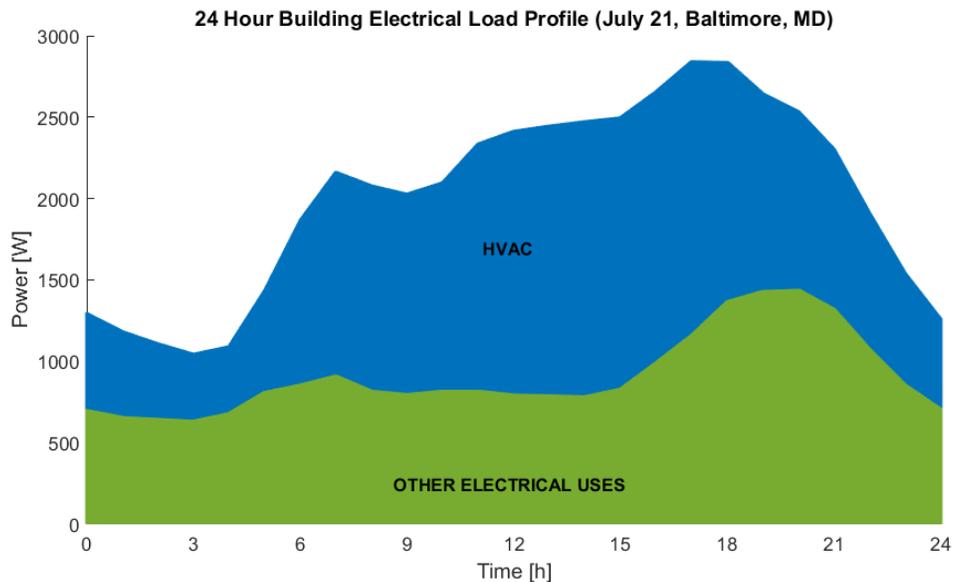

Figure 15. Thermal load of the prototype residential building in Baltimore on a typical summer day.

6.1 SYSTEM CONFIGURATION

Figure 16 shows the diagram of the modeled DPUTB-DSHP system. The refrigerant discharged from the DSHP's compressor can go to either a direct expansion condenser unit (i.e., a conventional air-water heat pump [AWHP]) or a coaxial coil heat exchanger (i.e., a conventional water-water heat pump [WWHP]), which is then connected with the helical heat exchanger in the annulus of the DPUTB. The chilled water (7°C) produced at the DSHP's evaporator is supplied to the building's HVAC system and the heat exchanger in the DPUTB's inner tank using a constant speed pump (P1). The DPUTB can be charged with the chilled water to store cooling energy with the PCM in the inner tank (by opening valves 1 and 4 and closing valves 2 and 3) or can be discharged to provide cold water to the building HVAC system (by opening valves 2 and 3 and closing valves 1 and 4). During the discharging operation, a variable speed pump (P2) dedicated to the DPUTB is operated to provide chilled water as needed for meeting the building's varying cooling loads. Another pump (P3) is used to circulate water between the DSHP's coaxial heat exchanger and the heat exchanger in the DPUTB's annulus. It is assumed that the leaving fluid temperature of the HVAC terminals in the building is maintained at 14°C.

17
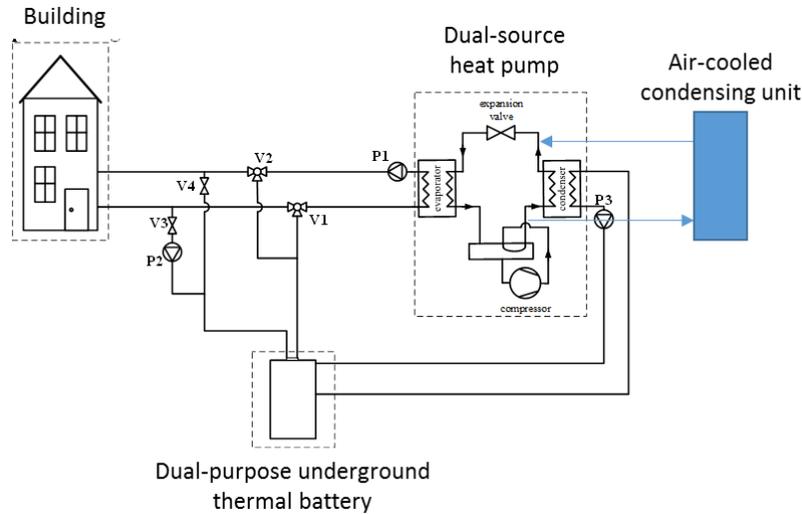
Figure 16. Diagram of the modeled DPUTB-DSHP system.

The experimentally validated DPUTB model is incorporated with a simplified model for the DSHP to simulate the operation of a DPUTB-DSHP system. The DSHP is modeled as a combination of two conventional heat pumps: an AWHP and a WWHP. Two curve fitting submodels were based on the heat pump models (type 927 and type 941) of the TRNSYS program (Klein et al. 2017). These heat pump models use performance curves of typical AWHP and WWHP units to predict their heating and cooling output and associated power consumption based on the inlet conditions at the condenser and the evaporator of these heat pumps.

In this case study, the maximum cooling capacity of the DSHP is 1.45 ton. It is assumed that DSHP uses a variable speed compressor so that it can adjust its cooling capacity based on control signals. The key parameters of the simulated DPUTB are listed in Table 2.

Table 2. Dimensions and key properties of the simulated dual-purpose underground thermal battery.

Property	Value	Unit
DPUTB dimensions		
Inner tank diameter	39	cm
Inner PVC shell thickness	0.55	cm
PCM blanket thickness	2.54	cm
Outer tank diameter	101.37	cm
Outer PVC shell thickness	0.82	cm
Height of the inner tank	609.60	cm
Height of the outer tank	609.60	cm
Inner shell thermal physical properties		
Material	PVC	–
Thermal conductivity	0.19	W/m K
Density	1380	kg/m^3
Specific heat	1000	J/kg K

Table 2. Dimensions and key properties of the simulated dual-purpose underground thermal battery (continued).

Property	Value	Unit
Outer shell thermal physical properties		
Material	HDPE	–
Thermal conductivity	0.50	W/m K
Density	950	kg/m^3
Specific heat	1900	J/kg K
Inner tank PCM thermal physical properties		
Melting point	12	°C
Heat of fusion	334	kJ/kg
Density (solid)	917.5	kg/m^3
Density (liquid)	998	kg/m^3
Thermal conductivity (solid)	2.25	W/m K
Thermal conductivity (liquid)	0.6	W/m K
Specific heat (solid)	2027	J/kg K
Specific heat (liquid)	4182	J/kg K
Annulus PCM thermal physical properties		
Melting point	14	°C
Heat of fusion	160	kJ/kg
Density	1118	kg/m^3
Thermal conductivity (solid)	0.1489	W/m K
Thermal conductivity (liquid)	0.1596	W/m K
Specific heat (solid)	3000	J/kg K
Specific heat (liquid)	2740	J/kg K
Soil thermal physical properties		
Thermal conductivity	1.70	W/m K
Density	1602	kg/m^3
Specific heat	2100	J/kg K

The UA values of the heat exchangers in the inner tank and the annulus are calculated as a function of mass flow in each heat exchanger, as expressed in Eq. (13).

$$UA = 5000 \cdot \dot{m},$$ (13)

where $\dot{m}$ is the mass flow rate of the heat carrier fluid in the heat exchanger (kg/s) and UA is in W/°C.

The hourly cooling load of a residential building in Baltimore was predicted with the US Department of Energy's (DOE's) prototype model for residential building, a single-family detached house (DOE 2014). The hourly cooling load is used as an input to the system simulation. The prototype residential building uses a conventional HVAC system, which includes an air conditioner with a nominal coefficient of performance (COP) of 3.97 and a gas furnace with an efficiency of 0.78. The electric load profile and power consumption of the prototype residential building were used as a baseline to be compared with that resulting from using the DPUTB-DSHP system.

6.2 CONTROL STRATEGY

The control strategy of the DPUTB-DSHP system is shown in Figure 17, and descriptions of various operating modes are listed in Table 3. The operation mode at a given time is determined with the following procedures depending on whether the current time is on-peak or off-peak.

- If the current time is on-peak, check whether the DPUTB inner tank water temperature is lower than the melting point of the PCM inside the inner tank.
  - o If so, only use the stored cooling energy in the DPUTB to meet the cooling demand of the building (mode 7).
  - o If not, check whether the ambient air temperature is lower than 26.7 °C.
    - If yes, operate DSHP as ASHP to meet the cooling demand (mode 1).
    - Otherwise, operate DSHP as a GHP to meet the cooling demand (mode 4).

- If the current is off-peak, operate DSHP as an ASHP if the ambient air temperature is lower than 26.7°C, otherwise operate DSHP as a GSHP.

- In each case (ASHP or GSHP), check whether the DPUTB is fully charged.
  - o If yes, operate DSHP to meet the cooling demand (mode 1 or mode 4).
  - o Otherwise, check whether the cooling demand is lower than the cooling capacity of the DSHP.
    - If yes, run DSHP to meet the cooling demand and charge DPUTB (mode 2 or mode 5).
    - Otherwise, run DSHP at its maximum capacity and together with discharging DPUTB to meet the cooling demand (mode 3 or mode 6).

The cooling capacity of the DSHP is adjusted at each time step based on the difference between the targeted whole building electric demand and the sum of the electric demands of all the non-HVAC end uses in the building at the time step. The difference in the electric demand is the allowed power draw of the DSHP, which can be translated to the allowed cooling capacity of the DSHP at the time step based on the efficiency of the DSHP. It is assumed that when the allowed cooling capacity of the DSHP is lower than 55% of its maximum capacity, the DSHP is turned off, and the building's cooling demand is met solely by the stored cooling energy in the DPUTB.
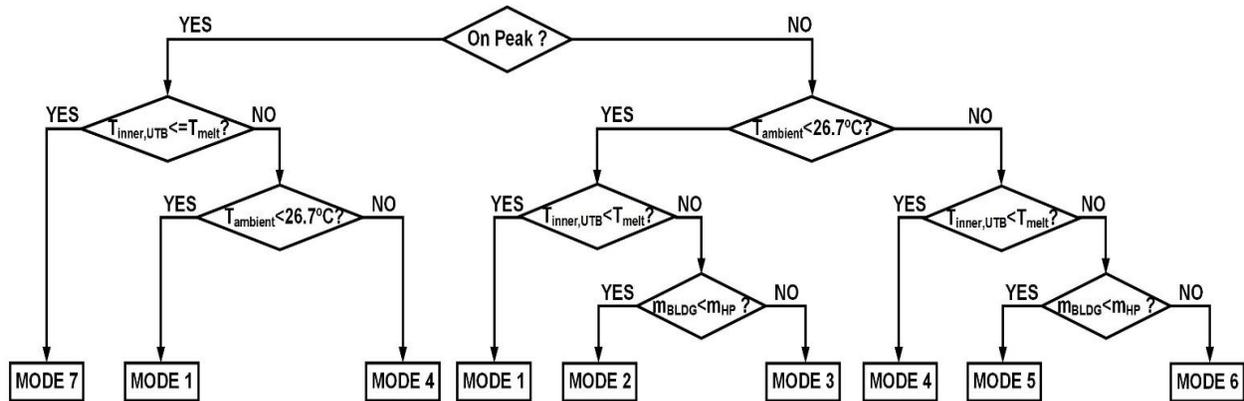

Figure 17. Strategies for determining the operation mode of the DPUTB-DSHP.

Table 3. Description of each operating mode of the integrated heat pump and thermal energy storage system.

Mode	Description
1	Heat pump on (air source), DPUTB off
2	Heat pump on (air source), DPUTB charging

| 3	Heat pump on (air source), DPUTB discharging
4	Heat pump on (ground source), DPUTB off
5	Heat pump on (ground source), DPUTB charging
6	Heat pump on (ground source), DPUTB discharging
7	Heat pump off, DPUTB discharging

6.3 SIMULATION RESULTS

The simulation results on a typical summer day (July 21) are shown in Figures 18 to 20. Figure 18 clearly shows that the building's electric load profile is flattened by DPUTB-DSHP system. Compared with the electric load profile resulting from using the conventional HVAC system, the DPUTB-DSHP system reduces the peak electric demand during the peak hours—from 10:00 to 20:00 (Baltimore Electric and Gas Company 2018)—by 37%. The DPUTB-DSHP system operates in the following different modes during the day:

- From 0:00 to 10:00, because of the relatively low ambient temperature, the DSHP operates as an ASHP to provide space cooling to the building and charge the DPUTB. As shown in Figure 19, the solid fractions of the PCMs in both the inner tank and annulus are increasing (i.e., the PCMs are frozen) during this period. On the other hand, the water temperature in the annulus barely changes due to the insulating effect of the PCM wrapping around the inner tank. Figure 19 shows that the capacity fraction of the DSHP (indicated by the dotted yellow line) ranges from 70% to 100% of its maximum capacity.

- From 10:00 to 14:00, the DPUTB is still being charged while the DSHP switches to GHP (i.e., rejecting heat to the annulus of the DPUTB) because the ambient air temperature is higher than the threshold (26.7°C). Due to heat rejection from the DSHP, the water temperature of the annulus increases, and the slopes of the solid fraction of the PCMs decrease. The capacity fraction of the DSHP is maintained at 80% as shown in Figure 20.

- From approximately 14:00 to 17:00, the building's cooling demand exceeds the maximum cooling capacity of the DSHP. Therefore, the DPUTB is discharged to release some cooling energy (indicated by the negative values of the blue line in Figure 20). The capacity fraction of the DSHP later drops from 80% to 55% due to the decreasing cooling demands.

- From 17:00 to 23:00, the DSHP is turned off, and the DPUTB releases stored cooling energy to meet the building's cooling demand. The solid fractions of the PCMs decrease as the stored cooling energy is released from the PCMs. The water in the annulus of the DPUTB is cooled by the surrounding soil (Figure 19).

- After 23:00, the capacity fraction of the DSHP increases above 55%, and the ambient temperature is lower than 26.7°C, so the DSHP runs as an ASHP again to provide space cooling to the building and charge the DPUTB as it does in the first period.
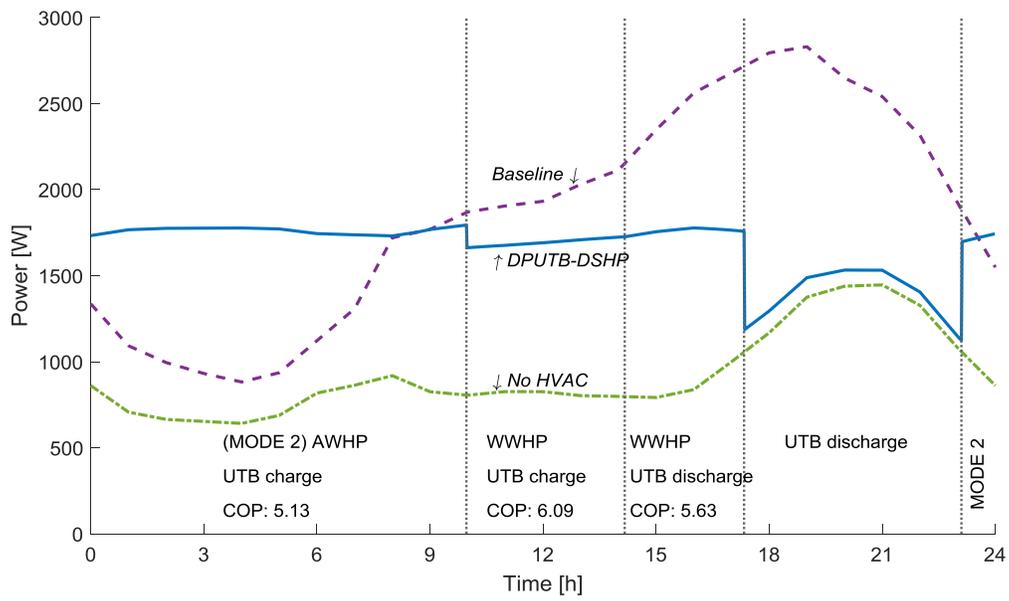
Figure 18. Electric load profile of the building.
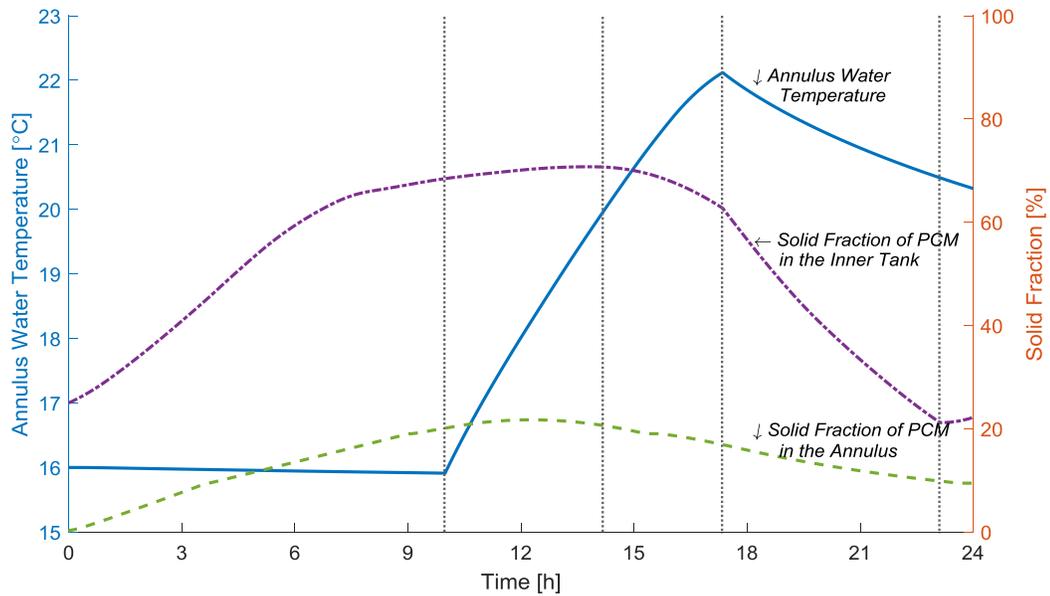
Figure 19. Water temperature in the annulus of the DPUTB and the solid fractions of PCMs in the inner tank and the annulus of the DPUTB.
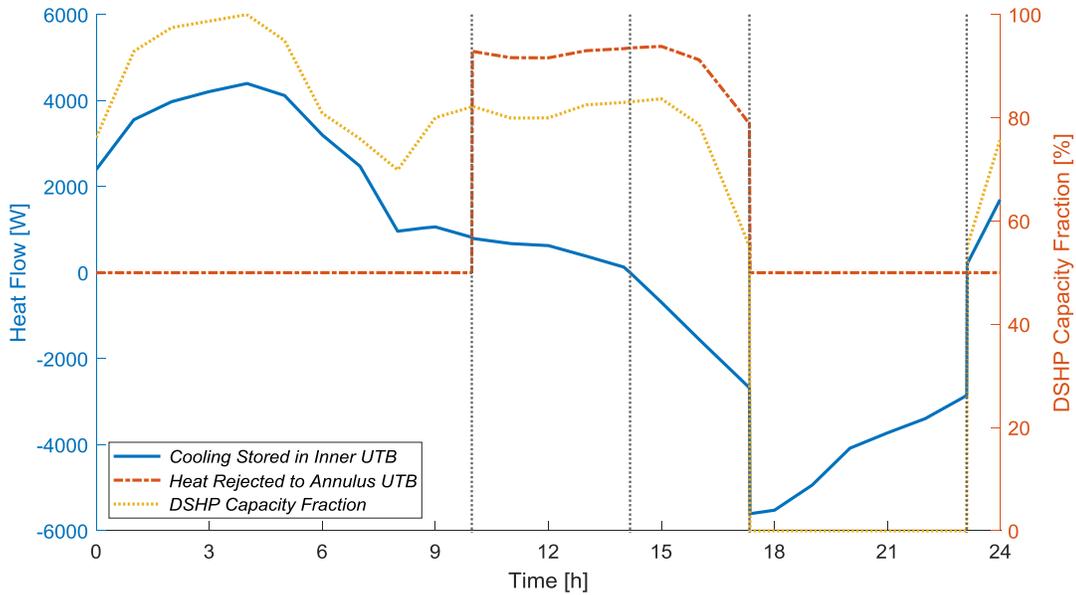
Figure 20. Thermal loads of the DPUTB in the inner tank and the annulus and the capacity fraction of the DSHP.

In addition to reducing the peak electric demand, the DPUTB-DSHP system reduces the building's power consumption by 11% (from 4.47 kWh to 3.99 kWh) compared with results using the conventional HVAC system. The energy savings result from the more efficient operation of the GHP when the ambient air temperature is high. The GHP's average operational efficiency, indicated by the COP, was ~6 when operating. The results of this case study indicate that the DPUTB-DSHP system can shift or level the electric load while reducing the power consumption of the simulated residential building.

7. CONCLUSIONS AND RECOMMENDATIONS FOR FUTURE WORK

The effort in the seedling project focused on the preliminary assessment of the technical feasibility of utilizing underground thermal energy storage and electric-driven heat pumps for enabling flexible behind-the-meter electric demand of buildings while meeting their thermal demands in an energy-efficient manner. A novel DPUTB as the UTES, which innovatively integrates a ground heat exchanger and underground thermal energy storage, was invented by ORNL in collaboration with Purdue University. A small-scale prototype of the DPUTB has been built and tested at ORNL.

A 1D transient numerical model of a novel thermal energy storage system, the DPUTB, has been developed and validated against the measured performance data of a small-scale prototype of DPUTB. The validated DPUTB model was incorporated into a heat pump system simulation to predict its performance under various operating conditions of a typical residential building in the United States.

The simulation results indicate that the DPUTB-DSHP system can shift or level the electric load profile of a typical residential building. Besides, the DPUTB also works as a low-cost ground heat exchanger to provide favorable entering water temperature for the heat pump's efficient operation. As a result, the DPUTB-DSHP system not only significantly reduces the building's electric demand during peak hours, but also saves energy compared with conventional HVAC systems. When deployed at large scale, this system could help mitigate the growing burden on the nation's electric grid, especially the duck-curve effect that results from increasing penetration of intermittent renewable power generation.

23

The following research and development work is recommended to move from the proved concept to practical implementations of DPUTB-DSHP system in homes and businesses:

- Improve the numerical model of DPUTB to account for seasonal variation of the soil temperature and heat fluxes on the ground surface.

- Optimize DPUTB design and its integration with the DSHP to maximize cost-effectiveness.

- Develop more intelligent controls for charging and discharging operations associated with the DPUTB-DSHP system.

- Investigate the performance of the DPUTB-DSHP system for heating operations. The configuration and size of the DPUTB, as well as the control strategy used with the DPUTB-DSHP system, need to be tailored for heating operations.

- Evaluate the long-term (e.g., seasonal or annual) performance of the DPUTB-DSHP system, particularly, investigating the impact of thermal buildup in the surrounding soil of the DPUTB.

- Assess the benefits and costs of the DPUTB-DSHP system and compare it with other HVAC integrated thermal energy storage systems for shifting buildings' electric loads.

REFERENCES

Baltimore Gas and Electric Company (2018). "Residential Optional Time-Of-Use – Electric Schedule RL." https://www.bge.com/MyAccount/MyBillUsage/Documents/Electric/P3_SCH_RL.pdf

Bojić, M., and Yik, F. (2005). Cooling energy evaluation for high-rise residential buildings in Hong Kong. *Energy and Buildings*, 37(4), 345–351.

CAISO (2013). "What the Duck Curve Tells Us about Managing a Green Grid." https://www.caiso.com/Documents/2011-08-10_ErrataLTPPTestimony_R10-05-006.pdf.

Cetin, K. S., Manuel, L., and Novoselac, A. (2016). Effect of technology-enabled time-of-use energy pricing on thermal comfort and energy use in mechanically-conditioned residential buildings in cooling dominated climates. *Building and Environment*, 96, 118-130.

Dominković, D. F., Gianniou, P., Münster, M., Heller, A., and Rode, C. (2018). Utilizing thermal building mass for storage in district heating systems: Combined building level simulations and system level optimization. *Energy*, 153, 949–966.

Hirmiz, R., Teamah, H. M., Lightstone, M. F., and Cotton, J. S. (2019). Performance of heat pump integrated phase change material thermal storage for electric load shifting in building demand side management. *Energy and Buildings*, 190, 103–118.

Klein, S. A. et al. (2017). "TRNSYS 18: A Transient System Simulation Program." Solar Energy Laboratory, University of Wisconsin, Madison. http://sel.me.wisc.edu/trnsys.

Martin, V., He, B., and Setterwall, F. (2010). Direct contact PCM–water cold storage. *Applied Energy*, 87(8), 2652–2659.

Muhieddine, M., Canot, E., and March, R. (2009). Various approaches for solving problems in heat conduction with phase change. *International Journal on Finite Volumes*, 19.

Olsthoorn, D., Haghighat, F., Moreau, A., and Lacroix, G. (2017). Abilities and limitations of thermal mass activation for thermal comfort, peak shifting and shaving: A review. *Building and Environment*, 118, 113–127.

Romanchenko, D., Kensby, J., Odenberger, M., and Johnsson, F. (2018). Thermal energy storage in district heating: Centralised storage vs. storage in thermal inertia of buildings. *Energy Conversion and Management*, 162, 26–38.

Turner, W. J. N., Walker, I. S., and Roux, J. (2015). Peak load reductions: Electric load shifting with mechanical pre-cooling of residential buildings with low thermal mass. *Energy*, 82, 1057–1067.

US Department of Energy (2014). "Building Energy Codes Program: Residential Prototype Building Models." https://www.energycodes.gov/development/residential/iecc_models.

US Energy Information Administration (2018). "Annual Energy Outlook 2018." Washington, DC. https://www.eia.gov/outlooks/aeo/2.